Journal of Power Sources 222 (2013) 253–260

Contents lists available at SciVerse ScienceDirect

Journal of Power Sources

journal homepage: www.elsevier.com/locate/jpowsour

Reforming of natural gas using coking-resistant catalyst for fuel cell system applications

Ning-Yih Hsu [a], King-Tsai Jeng [a,b,*]

[a] Institute of Nuclear Energy Research, Box 3–6, 1000 Wenhua Road, Longtan, Taoyuan 32546, Taiwan
[b] Research Division I, TIER, 7F, No. 16-8, Dehuei St., Taipei 10461, Taiwan

HIGHLIGHTS

- α-Al_2O_3 is a more stable catalyst support than γ-Al_2O_3.
- The Pt/CeO_2/α-Al_2O_3 catalyst is able to effectively eliminate coking problem.
- The CeO_2 coating layer provides excellent coking resistance for the catalyst.
- The CeO_2 coating layer also prevents catalyst from being pulverized.

ARTICLE INFO

Article history:
Received 28 June 2012
Received in revised form
24 August 2012
Accepted 27 August 2012
Available online 10 September 2012

Keywords:
Reforming catalyst
Catalyst support
Coking-resistance
Natural gas reforming
Autothermal reforming
Solid oxide fuel cell

ABSTRACT

A coking-resistant catalyst prepared using a novel catalyst support is characterized and its performance on reforming of natural gas for fuel cell system applications is investigated. Two key issues, i.e., the stability of catalyst under the reforming environment and deposition of carbon on the catalyst surfaces leading to deactivation, have to be resolved. The reforming operations are performed using a modified external autothermal reforming (ATR) approach. Desulfurized natural gas is used as a feedstock to avoid catalyst poisoning and air is exploited as an oxidant. It is found that the reforming catalyst is able to remain stable and free from pulverization at the desired operating conditions when α-Al_2O_3 is employed as a catalyst support in place of the commonly used γ-Al_2O_3 counterpart. In addition, the ceria (CeO_2)-assisted Pt catalyst coated on the α-Al_2O_3 support, i.e., Pt/CeO_2/α-Al_2O_3, is able to significantly eliminate the coking problem with a CH_4 conversion rate >99% and a generated H_2 concentration ~62% at 1073 K. A reaction mechanism is proposed to elucidate the coking-resistance of the catalyst, which also accounts for the stability of the catalyst. The reforming catalyst has been tested continuously for 2400 h and is still able to maintain a good operating condition.

1. Introduction

Solid oxide fuel cells (SOFCs) have been intensively investigated and developed for uses as an integral part of distributed power systems due to their high efficiencies, clean emissions, and operational quietness. Particularly, SOFC micro-combined heat and power (CHP) systems (<2 kW) for residential applications have become a focus of attention recently. This is due to high power efficiency (~60%) and high overall energy efficiency (~90%) with a triple function of power generating, heating, and cooling of the SOFC micro-CHP system, which is of special interest to the users. With the oil price rising to sky high and the need of substantial reduction in carbon emissions to the atmosphere, the demands for such high efficiency, clean power generating devices are ever-increasing.

Although a variety of fuels, such as hydrogen, natural gas, methane, alcohols, etc., can be applied to SOFCs, hydrogen gives the best performance of all. However, hydrogen gas needs to be generated by a suitable means to sustain the supply. Therefore, reforming of alternative fuels on site to provide hydrogen-rich gas for the SOFC stack is a common practice. Among them, reforming of natural gas, or methane [1,2], is the most promising one due to its abundance and easy supply. Natural gas contains mainly methane (>90%). With the aid of proper catalysts, methane undergoes catalytic reactions at high temperatures (e.g., >973 K) to generate hydrogen-rich gas, which can be directly applied to the SOFC stack.

The reforming catalyst must be stable and have high catalytic performance. In addition, it must be coking-resistant to ensure uninterrupted operation of the SOFC power system. There are three

* Corresponding author. Institute of Nuclear Energy Research, Box 3–6, 1000 Wenhua Road, Longtan, Taoyuan 32546, Taiwan. Tel.: +886 3 471 1400x5310; fax: +886 3 471 1412.
E-mail address: ktjeng@gmail.com (K.-T. Jeng).

0378-7753/$ – see front matter © 2012 Elsevier B.V. All rights reserved.
http://dx.doi.org/10.1016/j.jpowsour.2012.08.086

main reforming approaches, i.e., steam reforming (SR), partial oxidation reforming (POR), and autothermal reforming (ATR), which have been developed and employed in the fuel cell systems [3,4]. Briefly, SR is the reaction of fuel with steam to generate mainly carbon monoxide and hydrogen, i.e., syngas. It is an endothermic reaction and, therefore, external supply of heat to sustain the reforming reaction is required. POR is the reaction of fuel with a controlled amount of air (oxygen) to generate syngas. The reaction is exothermic and the generated heat is used to sustain the reforming reaction. Finally, ATR is the reaction of fuel with both steam and air (oxygen) to generate syngas. The reforming reaction is designed to be thermally neutral. In the present case, the reformer is aimed to be simple and compact for fuel cell system applications. The one-stage ATR approach [5–25], basically a combination of both SR and POR processes, has higher fuel efficiency than POR and better dynamic start-up capability than SR [4]. It also has the advantages of operating in a POR mode to quickly start up the reformer and the fuel cell stack as well as operating in an SR mode to generate more hydrogen if needed. Therefore, it is first chosen for carrying out performance tests.

Depending on the feedstock and the reforming approach used, a variety of catalysts, such as nickel- and platinum-based catalysts supported mainly on gamma alumina (γ-Al_2O_3), have been developed for such purposes [26–34]. However, the catalyst becomes less effective as unwanted side reactions may occur. A major cause of catalyst deactivation in reforming catalysts is coking [35–37], i.e., carbon is deposited on the surface of the catalyst resulting in catalyst failure. To solve this formidable problem, perhaps the best way is resorting to the use of effective coking-resistant catalysts. One of the most commonly employed approaches is exploiting a metal oxide, such as CeO_2, as a promoter [36–38] to a metal catalyst, e.g., nickel. This approach leads to the development of advanced reforming catalysts with better coking resistances and reforming performances [12]. Another problem has to be dealt with is the stability of the catalyst support. It was found from our previous experiments that the reforming at high operating temperature ($\sim$1073 K) for natural gas can easily cause breakdown and pulverization of the reforming catalyst, which generally uses low-temperature formed γ-Al_2O_3 support due to its inexpensiveness and porous structure. It is speculated that excessive accumulation of the deposited carbon in such porous structure might cause structural failure at high reforming temperatures. Thus, more robust and stable catalyst supports that can stand the reforming environment are urgently needed to be explored.

At present, reforming of natural gas is still a topic of intensive investigation for fuel cell system applications. Since the reformer investigated is a small-scale device, it must have somewhat different operating approaches from those of the industrial large-scale systems. In this study, a modified external autothermal reforming approach, using water and air instead of steam and pure oxygen, is employed. The developed small reformer is intended to be integrated with a 1 kW SOFC micro-CHP system.

2. Experimental

2.1. Preparation and characterization of reforming catalysts

The γ-Al_2O_3 species is purchased form Alpha Aesar in a form of 3.2×10^{-3} m tablet having a specific surface area of 1.75×10^5 m^2 kg^{-1} and containing 3% carbon. To obtain α-Al_2O_3, the γ-Al_2O_3 is put in an oven and blown with air. The temperature is then increased at a rate of 8.33×10^{-2} K s^{-1} (5 °C min^{-1}) to 1473 K followed by sintering for 6 h. Finally, the temperature is decreased at a rate of 8.33×10^{-2} K s^{-1} to room temperature. The CeO_2-assisted Pt catalyst coated on α-Al_2O_3 support, i.e., Pt/CeO_2/α-Al_2O_3, is prepared using the procedure as illustrated in Fig. 1, and the Ni/CeO_2/α-Al_2O_3 catalyst is prepared following a procedure similar to that of the Pt-based counterpart.

Characterizations of the prepared alumina supports and alumina-supported catalysts are carried out. The alumina supports are characterized using X-ray diffraction (XRD) (Bruker, D8 ADVANCE) technique to examine their crystalline structures, and both species are characterized using BET method to measure their surface areas. In addition, the catalyst layers are examined using a scanning electron microscopy/energy dispersive spectroscopy (SEM/EDS) instrument (JEOL, JSM-6510) to characterize the surface structures and elemental compositions. The morphology of the Pt/CeO_2/α-Al_2O_3 catalyst layer before and after reforming operation is illustrated using transmission electron microscopy (TEM).

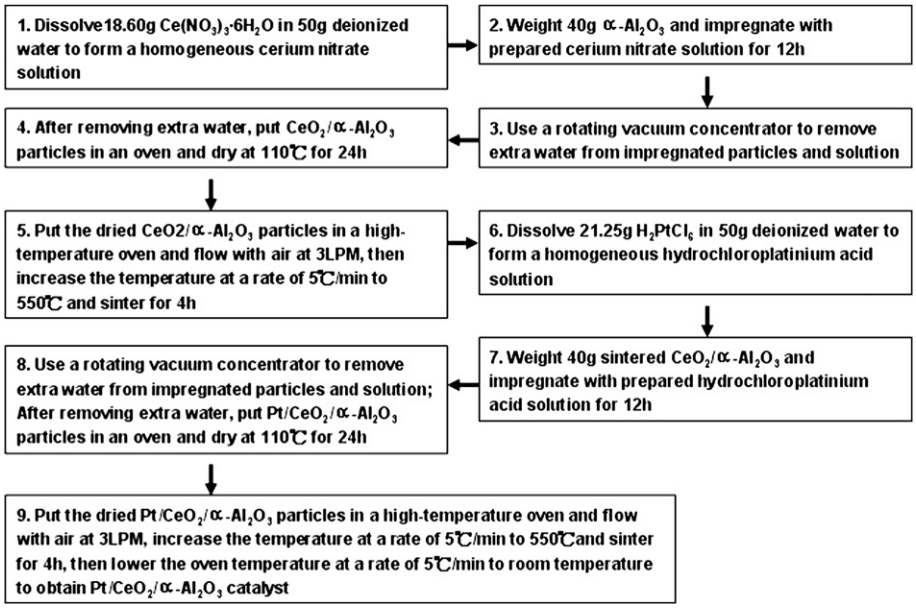

Fig. 1. Illustration of preparation procedure for Pt/CeO_2/α-Al_2O_3 catalyst.

2.2. Fabrication of reforming experimental apparatus

The reforming experimental setup is shown in Fig. 2. It is mainly composed of: (a) two gas mass flow controllers (Brooks, 5850E) for measuring flow rates of reactant gases; (b) a water syringe metering pump (KD Scientific, KDS100) for measuring water flow rate; (c) a vertical type high-temperature oven: programmable oven of 0.15 m in diameter and 0.35 m in length with operating temperature up to 1473 K; (d) a micro GC (Agilent, μ-GC 3000) for analysis of resultant gas composition. There is also a thermal couple for measuring reforming temperature and a gas-water separator at the reformed gas outlet. A catalyst column is properly installed within the high-temperature oven. In addition, a pressure gauge is arranged each at the inlet and the outlet of the reaction tube to monitor the pressure drop change during the experimental operations. A dryer is installed in front of the micro GC to remove moisture.

2.3. Reforming of natural gas with air using prepared catalyst

The desulfurized natural gas feedstock is obtained from CPC Corporation, Taiwan. It contains CH_4 (>95.0 mol%), butane (<2.0 mol%), S (<3.5 × 10^{-2} kg SM^{-3}), and N_2 (<1.0 × 10^{-3} kg SM^{-3}). The reforming operation is conducted using an autothermal reforming process with air as an oxidant. The reactants, i.e., natural gas, air, and water (instead of steam), are properly measured, well mixed and preheated before being sent into the catalytic reformer. Each experiment is carried out at specific fixed S/C (steam to methane) and O/C (oxygen to methane) ratios. The reforming temperature is controlled at 1073 K and the specific volume flow rate is 6.94 × 10^{-4} m^3 kg^{-1} s^{-1}.

The reforming reaction takes place in a U-shape quartz tube of 9.53 × 10^{-3} m (3/8″) inner diameter, which is properly installed in a programmable oven. Water is pumped into the reaction tube using a metering syringe pump through a 1.59 × 10^{-3} m (1/16″) inner tube. This inner tube is located as close to the inner wall of the quartz tube as possible allowing the input water to fall down along the wall of the quartz tube and readily evaporate into steam. At the same time, natural gas and air are sent into the reaction tube using mass flow controllers (MFCs) to accurately control the flow rate of each reacting species.

The reactants are well mixed before entering into the catalyst section filled with reforming catalyst of about 0.12 kg. After the reforming reaction, the products are passed through a water-gas separator and then directed to the SOFC stack. A part of the reformed gas stream is passed through a dryer and then directed to the micro GC analyzer for analysis of the product composition.

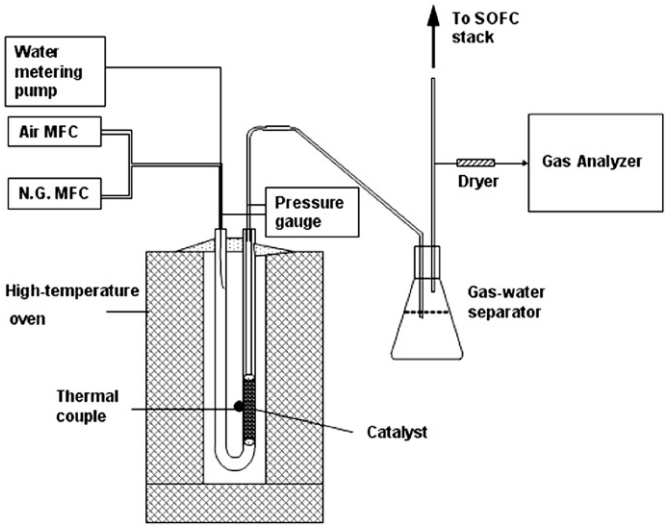

Fig. 2. Experimental setup for autothermal reforming of natural gas.

3. Results and discussion

3.1. On preparation and characterization of alumina-based catalyst supports

The phase change of alumina following the increase of heat treatment temperature is illustrated in Fig. 3. It can be seen that a variety of structures of the Al_2O_3 species can be formed [39]. Among them, the γ-Al_2O_3 formed at 723 K is the commonly used catalyst support due to its porous structure and high surface area. The α-Al_2O_3 formed at 1473 K and capable of standing high reforming temperature is the proposed new catalyst support used in this study. Basically, the purpose of calcinations for γ-Al_2O_3 is to remove the carbon species originally existing in it. This procedure also generates some porous structures on the alumina support which is favorable for the coating of a ceria layer. Both γ-Al_2O_3 and α-Al_2O_3 catalyst supports exist in a form of about 3 × 10^{-3} m tablet. The surface area of the former is 1.75 × 10^5 m^2 kg^{-1} and that of the later is about 6.0 × 10^4 m^2 kg^{-1}. It is obvious that both species possess microporous and meso-porous structures within the tablets so as to have such high surface areas. Characterizations on these two particular species are conducted and their XRD patterns are shown in Fig. 4. It can be seen that these two alumina species exhibit quite different characteristics due to different formation temperatures. The γ-Al_2O_3 has an indistinctive XRD pattern indicating mainly an amorphous structure. On the contrary, the α-Al_2O_3 obtained at a high formation temperature has distinctive sharp peaks suggesting a crystalline structure.

Since γ-Al_2O_3 is formed at a fairly low temperature, the characteristic of this material is having a porous structure with high surface area. Indeed, it is suitable for used as a catalyst support but only for low temperature applications. However, it is apparently not suitable for use with ATR of natural gas at an environment around 1023–1173 K due to its pulverization behavior, i.e., fine crushing of the reforming catalyst into powders, found in previous experiments. To stand the high temperature environment of the ATR operation, obviously α-Al_2O_3 is more robust in terms of structural strength at high reforming temperatures and thus more suitable to be employed as a catalyst support. The drawback can be that this species is denser in structure with a smaller surface area compared to that of γ-Al_2O_3.

However, it is found that the catalyst support is not the one that actually determines the catalyst surface area. As illustrated by the SEM image of the α-Al_2O_3 support shown in Fig. 5a, it can be seen that the uncoated α-Al_2O_3 support has a relatively smooth surface and the micropores and mesopores of the tablet are not clearly discernable. With the coating of a ceria layer on the α-Al_2O_3 support as a promoter for the catalyst as shown in Fig. 5b, the tablet surface becomes very rough but the specific surface area drops from 6.0 × 10^4 m^2 kg^{-1} to 2.0 × 10^4 m^2 kg^{-1}. It is obvious that the coating of CeO_2 layer has blocked the micro- and meso-porous structures inside the body of the catalyst support and decreased the surface area of α-Al_2O_3 support substantially. After further coating with Pt

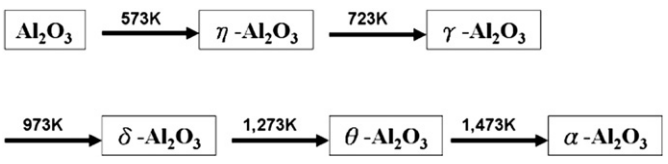

Fig. 3. Phase change scheme of the alumina species with increasing temperature.

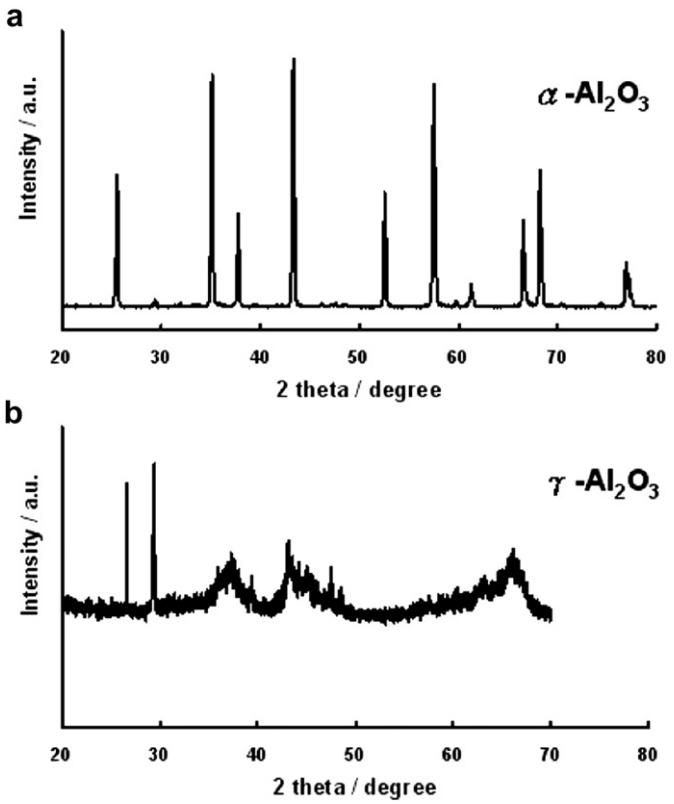

Fig. 4. XRD patterns of (a) α-Al_2O_3 and (b) γ-Al_2O_3.

and Ni catalyst as shown in Fig. 5(c) and (d), the surface area of each changes only slightly to 2.5×10^4 m^2 kg^{-1} and 1.9×10^4 m^2 kg^{-1}, respectively. Thus, the surface area for the Al_2O_3-supported catalyst at this stage is in fact mainly determined by the cerium oxide (CeO_2) layer coating instead of the original catalyst support. Although with some sacrifice in the surface area, this CeO_2 coating layer turns out to play an important role in providing the needed coking resistance to the catalyst as well as preventing the catalyst support from being broken down as will be further explained later in Section 3.4. On the contrary, the main function of the α-Al_2O_3 support is to keep the integrity of the catalyst at high operating temperatures to make the long-term operations possible.

Further comparison of the EDS results of prepared α-Al_2O_3, CeO_2/α-Al_2O_3 and Pt/CeO_2/α-Al_2O_3 materials as illustrated in Fig. 6, it clearly shows that the surface layers contain only Al, O, Ce and Pt elements. There are no undesirable foreign species present on the coating layers. This proves that the catalyst preparation procedure is reliable and the prepared catalyst is free from contamination.

3.2. On preparation and characterization of coking-resistant ATR catalyst

The coking-resistant catalysts are basically CeO_2-assisted Pt and Ni catalysts supported on α-Al_2O_3, prepared by subjecting to proper heat treatment. In general, the newly developed Pt/CeO_2/α-Al_2O_3 and Ni/CeO_2/α-Al_2O_3 catalysts are prepared using distinctive procedures somewhat different from that reported by Ferreira et al. [12]. In the first place, the alumina support is first converted to α-Al_2O_3 by proper heat treatment at 1473 K to ensure the stability of the prepared catalyst. Secondly, the ceria (CeO_2) layer and Pt catalyst layer are prepared using different coating procedures. Thirdly, the α-Al_2O_3 support coated with CeO_2 layer is not reduced with hydrogen at 1073 K. More precisely, the newly developed CeO_2-assisted catalysts have a two-layer coating structure with CeO_2 as an anchoring and promoting layer and Ni or Pt nano-particles as the true catalyst layer. The α-Al_2O_3 conversion and the CeO_2 coating processes are believed to be two critical steps to the success of preparing ATR catalysts with excellent coking resistances.

The resulting two key ATR reforming catalysts are 2%Pt/10%CeO_2/α-Al_2O_3 and 8.3%Ni/15%CeO_2/α-Al_2O_3, respectively, in terms of weight percentage. As shown earlier in Fig. 5, the ceria coating almost fully covers the α-Al_2O_3 support in a form of particle-packed thin layer as a catalyst promoter. This is totally different from the commonly used doping method, in which CeO_2 is doped into the bulk structure of the catalyst or support. It generates an ideal condition for the CeO_2-assisted catalyst. Furthermore, the use of low atomic ratios for the metal catalyst species ensures that the catalysts

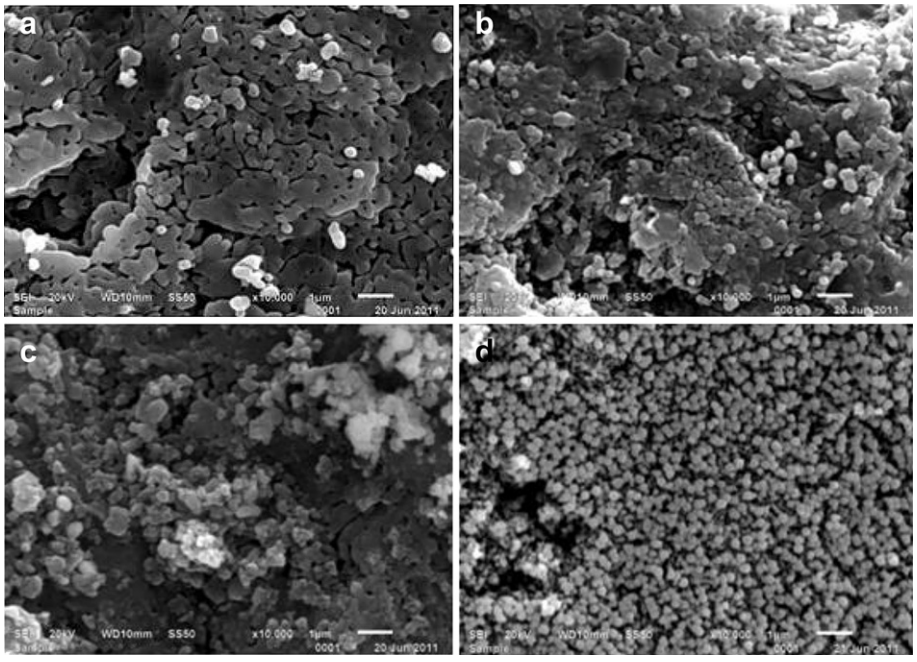

Fig. 5. SEM images of (a) α-Al_2O_3 (b) CeO_2/α-Al_2O_3 (c) Pt/CeO_2/α-Al_2O_3 and (d) Ni/CeO_2/α-Al_2O_3.

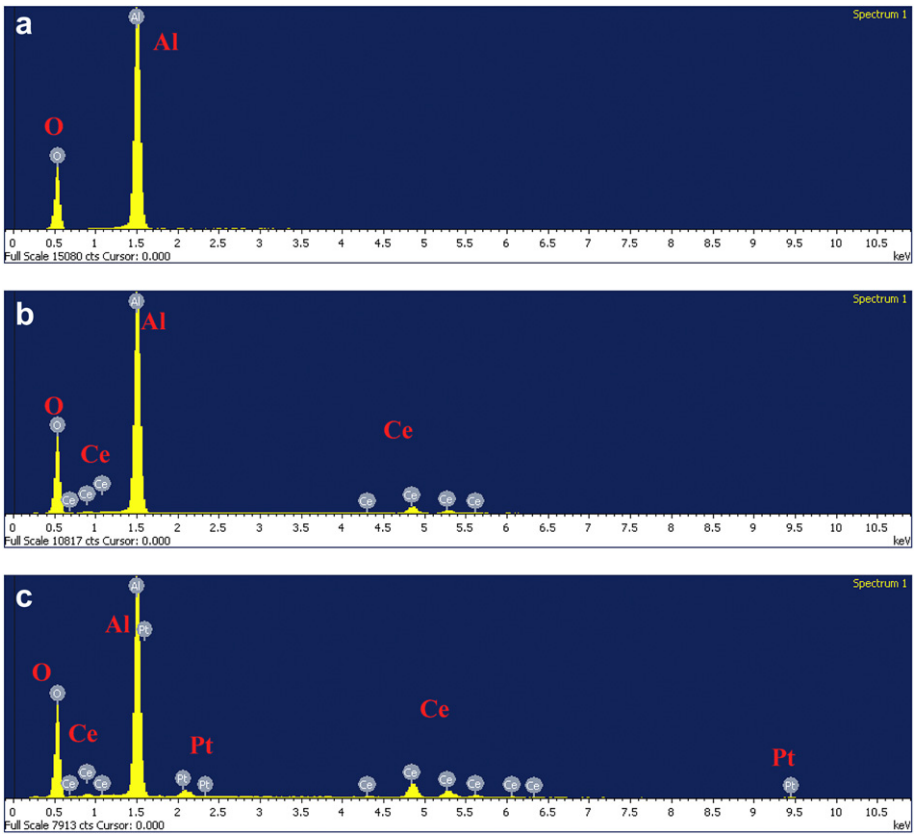

Fig. 6. Comparison of EDS results of prepared (a) α-Al_2O_3, (b) CeO_2/α-Al_2O_3 and (c) Pt/CeO_2/α-Al_2O_3 species.

are formed in nano-particles instead of bulk metal structures. Indeed, the Pt catalyst is more or less evenly distributed on the CeO_2 layer in a form of nanoparticle having a particle size of 5–10 nm. This nanocatalyst is definitely favorable for autothermal reforming of natural gas and will give rise to better catalytic performance. It is also aimed to make a cost-effective catalyst particularly for using precious Pt material. On the contrary, the higher loading of Ni catalyst results in a coarser particle-like coating layer.

3.3. Comparison on performances of ATR catalysts

Taking into account the feeding ratios of oxygen to methane (O/C) and steam to methane (S/C), the autothermal reforming of natural gas with air can be expressed as:

$$CH_4 + xO_2 + yH_2O + zN_2 \rightarrow (2 - 2x - y)CO + (2x + y - 1)CO_2 + (2 + y)H_2 + zN_2 \quad (1)$$

where $0 < x\ (=O/C) \leqq 1$, $0 < y(=S/C) \leqq 2$, and z is the ratio of nitrogen to methane [6]. Neglecting other minor fuel components and the effect of carbon deposition, the methane conversion rate (X) and the hydrogen yield (Y) can be expressed respectively as:

$$X\% = \frac{[CO]_o + [CO_2]_o}{[CO]_o + [CO_2]_o + [CH_4]_o} \times 100 \quad (2)$$

and

$$Y\% = \frac{[H_2]_o}{2[CH_4]_i + [H_2O]_i} \times 100 \quad (3)$$

where the subscripts o and i denote the concentration of each species measured at the reformer outlet and inlet, respectively. Briefly, the methane conversion rate in Eq. (2) is estimated from the amount of carbon converted divided by the total amount of carbon involved in the reforming reaction, while the hydrogen yield in Eq. (3) is calculated from the amount of hydrogen generated divided by the total amount of hydrogen contained in the feedstock. All the species concentrations can be measured accurately.

From the thermodynamic balance calculation, the reforming of methane with steam and oxygen should occur above 973 K. The end products should only contain H_2, CO, and CO_2 as well as some unreacted H_2O and CH_4. That is to say the carbon deposition phenomenon will not happen at such a high temperature. In practical reforming operation, this is not the case. In order to obtain the maximum hydrogen yield and avoid the occurrence of carbon deposition, the use of suitable reforming catalysts is a critical issue.

The ATR process should be thermally neutral, i.e., neither endothermic nor exothermic. However, in some cases it may not generate all the heat required for the reactions with specific feeding ratios, particularly when air and water are introduced into the feedstock in a small-scale reformer. Therefore, in practical operation some extra heat may be provided to sustain the reforming reaction at a desired high operating temperature for reforming of natural gas. This extra amount of heat can be readily obtained from waste heat of an SOFC stack through proper heat exchanging in a practical system. The use of air instead of pure oxygen for the reforming reaction is to avoid the use of an expensive air separation unit (ASU).

The performances of prepared Ni/CeO_2/α-Al_2O_3 and Pt/CeO_2/α-Al_2O_3 catalysts together with a commercial honeycomb catalyst (Pt–Rh–Pd/ceramic), commonly used in automobile catalytic converters, were compared on the autothermal reforming of natural gas. The honeycomb catalyst was purposely shaped to fit the configuration of the catalyst test tube. Based on the simulation

results of ATR for methane [6], it suggests that the reaction temperature of ATR plays an important role in determining the H_2 yield. Also, the conditions of higher steam/methane (S/C) ratio and lower oxygen/methane (O/C) ratio in conjunction with a higher reaction temperature have a trend to increase the H_2 yield. Therefore, the reforming temperature is fixed at 1073 K, and the reactant ratios are set at $S/C = 2$ and $O/C = 0.35$. The test results over a period of 7.2×10^3 s (120 min) operation are shown in Fig. 7, and the final gas outlet composition is listed in Table 1. It can be seen that the $Pt/CeO_2/\alpha$-Al_2O_3 catalyst outperforms the other two comparison counterparts with respect to the hydrogen yield. Moreover, the methane species is completely converted by the ATR process. This is due to the fact that Pt is a better catalyst for autothermal reforming of natural gas. It also indicates that the CeO_2 coating layer is playing a key role on the inhibition of carbon deposition.

Obviously, the random packing of the α-Al_2O_3-supported catalysts is favorable for prolonging the residence time of the reactants. However, the performance of the commercial honeycomb catalyst is not as good as expected. It may suffer from lacking of a CeO_2 coating layer, as well as having a larger void space in the reactant flow-through passage, leading to poorer reforming performance. As a result, about 4% of methane remains un-reacted at the reformer outlet. It should be pointed out that the generated hydrogen concentration is somewhat diluted by the presence of nitrogen due to the use of air as an oxidant in this case.

3.4. Reaction mechanism on coking-resistance of reforming catalyst

In fact, both Pt and Ni are effective catalysts for reforming of natural gas to generate hydrogen-rich gas. However, there are several reaction schemes that can result in carbon formation on the catalyst surfaces resulting in catalyst failure. Particularly, at high operation temperatures, the Boudouard reaction (c.f., Eq. (4)) and pyrolysis of methane (c.f., Eq. (5)) are considered to be the two most probable pathways for deposition of carbon on the catalyst, e.g., Pt, surfaces.

$$2CO + Pt \rightarrow CO_2 + C(Pt) \quad (4)$$

$$CH_4 + Pt \rightarrow 2H_2 + C(Pt) \quad (5)$$

where C(Pt) denotes carbon deposited on the Pt catalyst surface.

The application of CeO_2 as a catalyst promoter, such as CeO_2 doped Ni/Al_2O_3 [36–38], to cope with the catalyst coking problem is of particular interest in earlier studies. Souza et al. [40] reported that the CeO_2 is found to possess a large oxygen storage capability

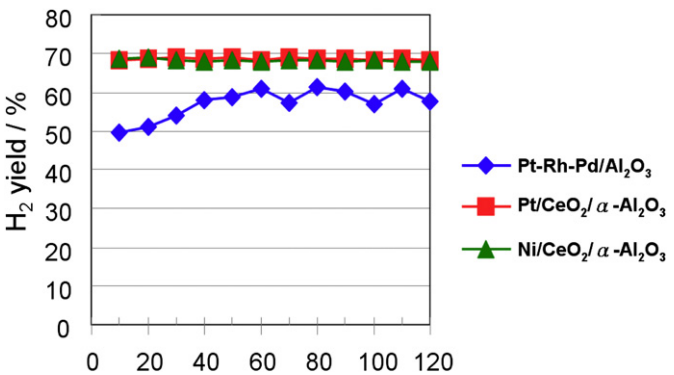

Fig. 7. Performance comparison for various catalysts on autothermal reforming of natural gas.

Table 1
Composition of reformed gas at ATR reformer outlet using various catalysts after 120 min operation.

Catalyst	Reformed gas composition					
	H_2 (%)	O_2 (%)	N_2 (%)	CH_4 (%)	CO (%)	CO_2 (%)
Honeycomb cat. (Pt–Rh–Pd/ ceramic)	57.5	0.0	12.0	4.0	19.8	5.6
$Pt/CeO_2/\alpha$-Al_2O_3	68.8	0.0	13.1	0.0	17.3	7.0
$Ni/CeO_2/\alpha$-Al_2O_3	68.0	0.0	13.1	0.0	17.1	6.8

(OSC), which is attributed to the ability of cerium to act as an oxygen buffer by storing/releasing oxygen due to the Ce^{4+}/Ce^{3+} redox couple. Since nickel is a catalyst known to easily cause carbon deposition during reforming operation, the OSC capacity is believed to be an essential property in order to keep the catalyst stable, as the oxygen storing/releasing allows a continuous removal of carbonaceous deposits from the metal surface.

Although the OSC model is interesting, it may not truly account for the real coking resistance in the reforming process. Since the reforming reaction occurs on the catalyst surface, it is the active oxygen species on the CeO_2 surface that plays a key role in the reforming reaction, instead of the oxygen stored in the bulk of CeO_2 species, which gives rise to excellent coking resistance of the catalyst. Thus, a reaction mechanism is proposed as illustrated in Fig. 8 to elucidate the reforming process with the removal of deposited carbon on the Pt catalyst. As can be seen a thin CeO_2 layer is coated on, rather than doped in, the α-Al_2O_3 support surface and on top of it Pt catalyst nano-particles are formed. In an oxygen-containing environment at high temperatures, active oxygen species are readily formed on the CeO_2 surface, which then readily spill over and react with the carbon deposited on the Pt catalyst leading to formation and removal of CO_2 and a clean catalyst surface. This process can be expressed as:

$$O_2 + CeO_2 \rightarrow CeO_2 \cdot 2(O)_s \quad (6)$$

$$CeO_2 \cdot 2(O)_s + C(Pt) \rightarrow CO_2 + CeO_2 + Pt \quad (7)$$

where $(O)_s$ denotes the active oxygen species formed on the CeO_2 surface.

The consumed active oxygen species are readily regenerated again on the CeO_2 surface through the Ce^{4+}/Ce^{3+} redox process with supplement of air in the feedstock. Obviously, the thin layer coating of CeO_2 used in this study is more favorable than the doped counterpart with respect to regeneration of the needed active oxygen species on the surface. Thus, it is the self-regenerative characteristic of the CeO_2 coating to produce active oxygen species on the surface, in an oxygen-containing environment at high temperatures, which helps to remove the deposited carbon from the Pt catalyst surface resulting in excellent coking resistance.

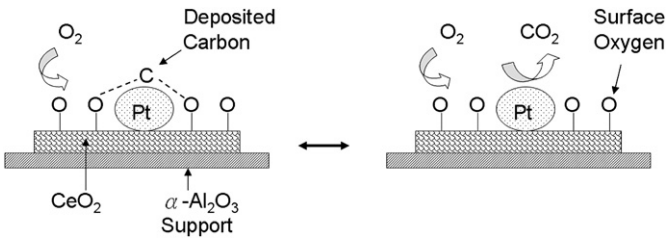

Fig. 8. The proposed reaction mechanism for $Pt/CeO_2/\alpha$-Al_2O_3 catalyst with coking resistance.

In fact, the role of the CeO_2 coating layer is more suitable to be regarded as a catalyst coking inhibitor or an anti-coking agent. The ATR process with sufficient oxygen in the feedstock is able to meet the need of the regenerative process for the formation of active oxygen species on the CeO_2 coating layer.

It is also depends on the harmoniously orchestrated mechanism of both CeO_2 and Pt species in the coating layer that results in a clean catalyst surface and an enhanced reforming efficiency. As results, the hydrogen yield reaches as high as 68.8% within the 7.2×10^3 s test period. In addition, no methane is detected at the outlet of the reformer indicating the natural gas is almost completely converted using the prepared $Pt/CeO_2/\alpha$-Al_2O_3 catalyst. It can be seen that the competing $Ni/CeO_2/\alpha$-Al_2O_3 species also exhibits a fairly good performance comparative to that of the $Pt/CeO_2/\alpha$-Al_2O_3 catalyst. Based on the proposed reaction mechanism, the enhanced performance efficiency of the reforming catalysts obviously can be attributed to the application of a CeO_2 layer as an effective catalyst coking inhibitor.

In addition, it is thought that the coking problem may be closely related to the breakdown of Ni/γ-Al_2O_3 catalyst, without applying a CeO_2 coating, as encountered in our previous studies. That is to say the deposition of carbon not only causes failure of catalyst but also breakdown of catalyst support structure. It was found that after a short period of operation this catalyst has lost its reforming activity and pulverized into much smaller particles covered with a black species. In the meantime, the small pipeline of the test device was found to cover with a black dust. Further examinations using EDS *analysis* revealed that the pulverized catalyst particles contains about 7.78% (atomic) of carbon and the black dust contains nearly 100% carbon indicating the occurrence of severe coking phenomenon. At a high reforming temperature, e.g., ~1073 K, the strength of the catalyst support structure will become much weaker than it is at room temperature. As a part of the natural gas reforming reaction may occur deep in the small porous structures of the catalyst support, the continuous accumulation of deposited carbon species eventually will exert a force that is large enough to accelerate fracture and breakdown of the catalyst support structure leading to totally failure of the reforming catalyst. With the coating of a CeO_2 layer as a coking inhibitor to the catalyst, Ni and Pt alike, such problem is effectively eliminated. In other words, the CeO_2 coating layer not only eliminates the coking problem but also prevents the catalyst from being broken down. Thus, the use of a CeO_2 coating layer to assist the catalyst in natural gas reforming is regarded to be effective and indispensable.

3.5. Long-term test of coking-resistant ATR catalyst

A long-term test for the Pt-based ATR catalyst incorporated with a ceria coating has been carried out for practical application purpose. The pressure drop of the test column is used to monitor the operating condition. By rule of thumb, a large pressure drop taking place during the operation indicates severe blockage of the catalyst packing section, which is generally caused by either pulverization of catalyst or deposition of carbon. Further examination of the gas outlet filter can clearly distinguish these two events. In addition, analysis of the composition of the reformed gas can tell if the catalyst works properly. The long-term test result of the $Pt/CeO_2/\alpha$-Al_2O_3 catalyst on autothermal reforming of natural gas at 1073 K is shown in Fig. 9. It can be seen that the outlet gas compositions of all species remain fairly stable over a period of 2400 h indicating the catalyst is in an excellent working condition. Even after such a long period of operation, a methane conversion rate >99% is achieved with the generated hydrogen having a high concentration of about 62% suitable for small-scale SOFC system application.

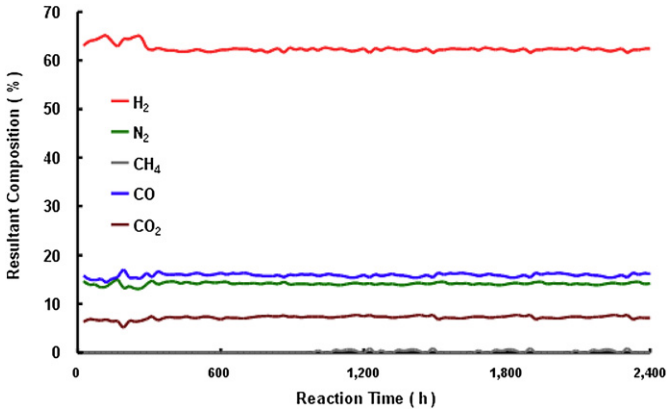

Fig. 9. A long-term test result of $Pt/CeO_2/\alpha$-Al_2O_3 catalyst for ATR of natural gas with air.

During the operation, the catalyst column maintains steady with a pressure drop of around 460 mbar. In addition, no carbon deposition is found by visual examination of the gas filter and the catalyst packing suggesting the catalyst is indeed coking-resistant. The results of the long-term operation, as compared to previously reported results [40], prove that surface coating of CeO_2 is a better approach than doping in the preparation of reforming catalyst as it can fully utilize the coated species. Overall, the successful long-term operation is made possible by the use of both stable α-Al_2O_3 catalyst support and effective CeO_2-assisted catalyst with high coking resistance.

Furthermore, the TEM pictures show that there are almost no changes in the shapes and sizes of the Pt catalysts before and after the ATR operation as illustrated in Fig. 10. In general, the lighter species Ce in its oxide form shows a brighter color while the heavier Pt element exhibits a darker color on the coating layer. In addition, the CeO_2 with a larger amount of coating has a layer structure,

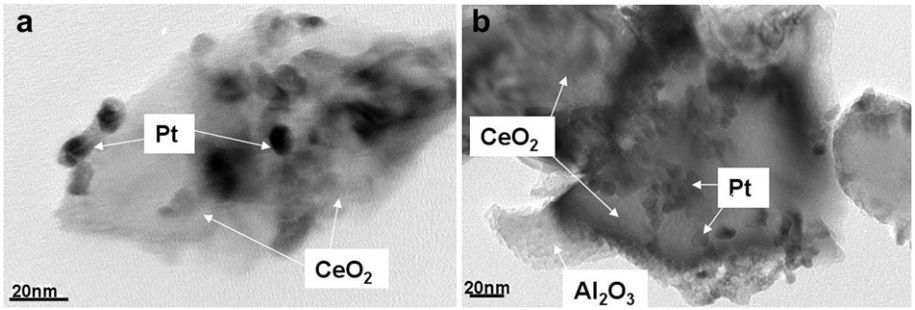

Fig. 10. TEM images of $Pt/CeO_2/\alpha$-Al_2O_3 catalyst (a) before and (b) after ATR of natural gas.

while the Pt catalyst with a smaller amount of coating exists in a particle-like deposit. Comparison of the EDS results (c.f. Fig. 6) also indicates that no contaminated species are present on the coating layers. Therefore, it is relatively easy to identify the CeO_2 and Pt species in the catalyst coating layer. Overall, the particle sizes of the Pt catalyst remain almost the same at around 5–10 nm. More interestingly, it can be seen that where the CeO_2 promoter layer is clearly discernable the Pt catalyst particles are uniformly sitting on top of it. Where the alumina support is not covered with CeO_2, there is no presence of Pt particles. This peculiar phenomenon directly demonstrates the combined effect of these two species on the catalytic reforming of natural gas.

4. Conclusions

Generation of hydrogen-rich gas via autothermal reforming of natural gas with air is investigated for 1 kW SOFC micro-CHP system application. Two key issues encountered previously, i.e., breakdown and pulverization of γ-Al_2O_3-supported catalyst under the ATR environment at around 1073 K as well as deposition of carbon on the catalyst, have been resolved. The former is solved by direct transformation of γ-Al_2O_3 support into the α-Al_2O_3 form by subjecting to proper heat treatment before coating the cerium oxide and catalyst layers. The later is resolved by developing a coking-resistant catalyst, i.e., Pt/CeO_2/α-Al_2O_3. This catalyst has been successfully demonstrated for ATR of natural gas with air that exhibits excellent coking-resistance and reforming performance. Although with some sacrifice in catalyst surface area, surface coating of CeO_2 is believed to be a better approach than doping the catalyst support in the preparation of reforming catalyst with respect to more efficient utilization of the coating layer. The proposed reaction mechanism suggests that, at high reforming temperatures, the CeO_2 coating layer plays a key role to effectively eliminate the coking problem of the reforming catalyst as well as prevents the catalyst support from being pulverized. A hydrogen concentration of $\sim$62% is obtained with a methane conversion rate $>$99% at 1073 K for more than 2400 h in operation.

Acknowledgements

We gratefully appreciate the financial supports from National Science Council (NSC) and Institute of Nuclear Energy Research (INER), both of Taiwan, for the performance of this work under contract number: AEE0304.

References

[1] T. Zhang, M.D. Amiridis, Applied Catalysis A: General 167 (1998) 161–172.
[2] T. Koerts, M.J.A.G. Deelen, R.A.V. Santen, Journal of Catalysis 138 (1992) 101–114.
[3] J. Larminie, A. Dicks, in: Fuel Cell Systems Explained, second ed. Wiley, West Sussex, 2003.
[4] G. Hoogers, in: G. Hoogers (Ed.), Fuel Cell Technology Handbook, CRC Press, Boca Raton, 2003, pp. 5.8–5.12.
[5] M.H. Akbari, A.H. Sharafian Ardakani, M. Andisheh Tadbir, Chemical Engineering Journal 166 (2011) 1116–1125.
[6] W.H. Chen, M.R. Lin, J.J. Lu, Y. Chao, T.S. Leu, International Journal of Hydrogen Energy 35 (2010) 11787–11797.
[7] C.N. A'vila-Neto, S.C. Dantas, F.A. Silva, T.V. Franco, L.L. Romanielo, C.E. Hori, A.J. Assis, Journal of Natural Gas Science and Engineering 1 (2009) 205–215.
[8] A.E.A.M. Souza, L.J.L. Maciel, N.M. Lima Filho, C.A.M. Abreu, Catalysis Today 149 (2010) 413–417.
[9] J.A.C. Ruiz, F.B. Passos, J.M.C. Bueno, E.F. Souza-Aguiar, L.V. Mattos, F.B. Noronha, Applied Catalysis A: General 334 (2008) 259–267.
[10] M.L. Rodrigueza, D.E. Ardissoneb, M.N. Pederneraa, D.O. Borioa, Catalysis Today 156 (2010) 246–253.
[11] V. Modafferi, G. Panzera, V. Baglio, F. Frusteri, P.L. Antonucci, Applied Catalysis A: General 334 (2008) 1–9.
[12] A.P. Ferreira, D. Zanchet, J.C.S. Araujo, J.W.C. Liberatori, E.F. Souza-Aguiar, F.B. Noronha, J.M.C. Bueno, Journal of Catalysis 263 (2009) 335–344.
[13] S.H.D. Lee, D.V. Applegate, S. Ahmed, S.G. Calderone, T.L. Harvey, International Journal of Hydrogen Energy 30 (2005) 829–842.
[14] H.M. Wang, Journal of Power Sources 177 (2008) 506–511.
[15] T. Mendiara, J.M. Johansen, R. Utrilla, A.D. Jensen, P. Glarborg, Fuel 90 (2011) 1370–1382.
[16] J.S. Lisboa, L.E. Terra, P.R.J. Silva, H. Saitovitch, F.B. Passos, Fuel Processing Technology 92 (2011) 2075–2082.
[17] K. Faungnawakij, N. Viriya-empikul, W. Tanthapanichakoon, International Journal of Hydrogen Energy 36 (2011) 5865–5874.
[18] A. Gutierrez, R. Karinen, S. Airaksinen, R. Kaila, A.O.I. Krause, International Journal of Hydrogen Energy 36 (2011) 8967–8977.
[19] X. Karatzas, K. Jansson, A. González, J. Dawody, L.J. Pettersson, Applied Catalysis B: Environment 106 (2011) 476–487.
[20] Z. Mosayebi, M. Rezaei, A.B. Ravandi, N. Hadian, International Journal of Hydrogen Energy 37 (2012) 1236–1242.
[21] K.-M. Kang, I.-W. Shim, H.-Y. Kwak, Fuel Processing Technology 93 (2012) 105–114.
[22] M. Simeone, L. Salemme, L. Menna, International Journal of Hydrogen Energy 37 (2012) 9049–9057.
[23] W.-H. Lai, M.-P. Lai, R.-F. Horng, International Journal of Hydrogen Energy 37 (2012) 9619–9629.
[24] M. Rezaei, F. Meshkani, A.B. Ravandi, B. Nematollahi, A. Ranjbar, N. Hadian, Z. Mosayebi, International Journal of Hydrogen Energy 36 (2011) 11712–11717.
[25] K. Aasberg-Petersen, I. Dybkjær, C.V. Ovesen, N.C. Schjødt, J. Sehested, S.G. Thomsen, Journal of Natural Gas Science and Engineering 3 (2011) 423–458.
[26] C. Song, Catalysis Today 77 (2002) 17–49.
[27] S.T. Yong, K. Hidajat, S. Kawi, Journal of Power Sources 131 (2004) 91–95.
[28] V.V. Galvita, G.L. Semin, V.D. Belyaev, V.A. Semikolenov, P. Tsiakaras, V.A. Sobyanin, Applied Catalysis A 220 (2001) 123–127.
[29] E.C. Wanat, K. Venkataraman, L.D. Schmidt, Applied Catalysis A: General 276 (2004) 155–162.
[30] J. Sun, X. Oiu, F. Wu, W. Zhu, W. Wang, S. Hao, International Journal of Hydrogen Energy 29 (2004) 1075–1081.
[31] D.K. Liguras, K. Goundani, X.E. Verykios, Journal of Power Sources 130 (2004) 30–37.
[32] K. Sato, Y. Tanaka, A. Negishi, T. Kato, Journal of Power Sources 217 (2012) 37–42.
[33] T. Suzuki, H. Iwanami, O. Iwamoto, T. Kitahara, International Journal of Hydrogen Energy 26 (2001) 935–940.
[34] V. Recupero, L. Pino, A. Vita, F. Cipiti, M. Cordro, M. Lagana, International Journal of Hydrogen Energy 30 (2005) 963–971.
[35] J. Xu, M. Saeys, Journal of Catalysis 242 (2006) 217–226.
[36] Y.F. Yu-Yao, J.T. Kummer, Journal of Catalysis 106 (1987) 307–312.
[37] Y. Zhang, S. Anderson, M. Muhammed, Applied Catalysis B: Environment 6 (1995) 325–337.
[38] N. Loasiripojana, W. Sutthisripok, S. Assabumrungrat, Chemical Engineering Journal 112 (2005) 13–22.
[39] R.B. Bagwell, G.L. Messing, Journal of American Ceramic Society 82 (1999) 825–832.
[40] M.M.V.M. Souza, S. Sabino, F.B. Passos, L.V. Mattos, F.B. Noronha, M. Schmal, Studies in Surface and Catalysis 147 (2004) 253–258.